Composites Science and Technology 71 (2011) 931–937

Contents lists available at ScienceDirect

Composites Science and Technology

journal homepage: www.elsevier.com/locate/compscitech

Mechanical and electrical properties of polymer-derived Si–C–N ceramics reinforced by octadecylamine – Modified single-wall carbon nanotubes

D. Shopova-Gospodinova [a,*], Z. Burghard [a], T. Dufaux [b], M. Burghard [b], J. Bill [a]

[a] Institut für Materialwissenschaft, Universität Stuttgart, Heisenbergstraße 3, 70569 Stuttgart, Germany
[b] Max-Planck-Institut für Festkörperforschung, Heisenbergstrasse 1, 70569 Stuttgart, Germany

ARTICLE INFO

Article history:
Received 11 November 2010
Received in revised form 21 February 2011
Accepted 24 February 2011
Available online 1 March 2011

Dedicated to Professor Wolfgang Laqua on the Occasion of his 75th Birthday

Keywords:
A. Carbon nanotubes
A. Polymer-matrix composites
B. Mechanical properties
B. Electrical properties

ABSTRACT

Polymer-derived Si–C–N ceramics reinforced by homogeneously distributed octadecylamine–functionalized single-walled carbon nanotubes (SWCNTs) were synthesized using a casting process, successive pressureless cross-linking and thermolysis. We find that the incorporation of even small amounts of modified SWCNTs leads to a remarkable improvement of mechanical and electrical transport properties of our composites. In particular, we find twofold enhancement of fracture toughness. The Youngs modulus and the hardness show increase by ~30% and 15%, respectively. Furthermore, the electrical conductivity was found to increase more than five orders of magnitude even for a tube content of 0.5 wt.%.

1. Introduction

Ceramics based upon polymer-derived silicon carbonitride (Si–C–N) have attracted great interest for structural applications due to their low density, high hardness and elastic modulus, extraordinary chemical stability, and high creep resistance at elevated temperatures [1–5]. These excellent properties are reached through cross-linking and pyrolysis of organosilicon precursor polymers, leading to ceramics with high purity, controlled structure and chemical composition [1,6,7]. Depending on the chemical nature of the starting precursor and pyrolysis conditions, different ceramics whose atomic structure ranges from fully amorphous to nanocrystalline can be obtained [8]. Moreover, this synthesis route enables forming ceramics bodies into small scales and complex shapes, which is of strong relevance for many technological applications. However, like all ceramics, the resulting non-oxide material suffers from low fracture resistance and poor electrical conductivity [9–11]. Consequently, strategies to improve the fracture resistance and electrical conductivity of these materials are needed in order fully exploit their application perspectives.

Enhanced fracture resistance of ceramic materials has been achieved, among other approaches, via tailoring the microstructure by incorporating a second phase in the form of particles or fibers. Carbon nanotubes (CNTs) have proven particularly useful for this purpose [12,13], owing to their extraordinary mechanical [14–17], thermal [18] and electrical properties [19], as well as their low weight and high aspect ratio. There are numerous examples of enhanced electrical conductivity upon incorporation of carbon nanotubes in polymer matrices [20]. For instance, Ionescu et al. have attained good electrical conductivity through incorporation of 5 vol.% multi-wall carbon nanotubes (MWCNT) into polysilazane-derived Si–C–N ceramic.

Up to date, several mechanical studies of CNTs/polymer-derived ceramic composites have been reported, in most cases comprising multi-wall carbon nanotubes (MWCNTs) as reinforcing elements [21,22]. In one case, the MWCNTs were mixed into a Si–C–N ceramic precursor solution, followed by catalytic cross-linking and pressure-assisted pyrolysis at 1000 °C [21]. In this manner, a substantial increase in Young's modulus, hardness and contact-damage resistance was achieved for a MWCNTs content of ~6 vol.%. In a related work [22], MWCNTs were ultrasonically dispersed in a liquid polysilazane precursor polymer, with subsequent casting, pressure less cross-linking and thermolysis at 1000 °C. Preliminary investigations of the fracture toughness of thus obtained composites using a thermal loading method revealed that the extent to which the incorporated nanotubes enhance the mechanical properties depends strongly on their structural characteristics, in particular their aspect ratio [23]. Recently, we have utilized single-wall carbon nanotubes (SWCNTs) for the reinforcement of

* Corresponding author. Tel.: +49 711 685 61967; fax: +49 711 689 1010.
E-mail address: mwishopova@imw.uni-stuttgart.de (D. Shopova-Gospodinova).

0266-3538/$ - see front matter © 2011 Elsevier Ltd. All rights reserved.
doi:10.1016/j.compscitech.2011.02.013

Si–C–N polymer-derived ceramics, and found that the increase of Young's modulus increases with the dispersion degree of the nanotubes inside the amorphous matrix [24]. However, while it is well-documented that the incorporation of SWCNTs into polymer-derived amorphous ceramics can enhance their mechanical performance and electrical conductivity, detailed studies of the fracture toughness are very limited. Recent results reveal that the incorporation of MWCNT into Si–C–N amorphous ceramics and the formation of CNT–matrix interfaces lead to 25% increase of the fracture toughness [23]. Due to their small diameter SWCNTs basically provide a means to increase the interface area without changing carbon nanotubes weight fraction. A promising route toward well-separated and homogeneously distributed SWCNTs relies upon appropriate chemical functionalization of the tubes [25]. The work of Gojny et al. [26] has demonstrated that the presence of carboxylic groups on the surface leads to a better dispersion of the nanotubes in an epoxy system. Especially attractive is the use of polymers in the nanotube functionalization. In this context, Hill et al. have attached a polystyrene copolymer to SWCNTs, which then could be homogeneously dispersed within a polystyrene matrix [27].

Here, we report the synthesis of a polymer-derived Si–C–N amorphous ceramic, reinforced by octadecylamine-functionalised SWCNTs. It is demonstrated that the presence of long alkyl chains on the tubes promotes the efficient disintegration of nanotube bundles into individual nanotubes, and their dispersion inside the polymer precursor matrix. The major aim of this study was to explore the influence of concentration and agglomeration state of the SWCNTs on the mechanical and electrical properties of the resulting composites. To this end, the hardness and Young's modulus of the composites were determined by nanoindentation technique, while the fracture toughness was determined by measuring the crack opening displacement (COD) of indentation cracks.

2. Experimental

2.1. Materials and processing of composites

The SWCNT-reinforced polymer-derived Si–C–N ceramics were prepared following the procedure illustrated in Fig. 1. Commercial liquid poly(ureamethylvinyl)silazane (Ceraset, KION, USA) was used as starting precursor polymer. Octadecylamine-functionalised SWCNTs (P5-SWCNTs) were purchased from Carbon Solutions, Inc., USA, 60–70 wt.% SWCNT loading) and utilized without any further purification. 1,2-Dichlorobenzene (Aldrich, 99.9%) was used as a solvent. The synthesis was performed by a standard Schlenk technique under argon. In the first step, the required amount of P5-SWCNT was dispersed for 15 min in 1 ml of 1,2-dichlorobenzene using an ultrasonic bath (SONOREX RK 52H, 140W, BANDELIN electronic). In order to obtain 0.5, 1 and 2 wt.% P5-SWCNT content, the calculated amounts of degassed Ceraset were added to the solution of P5-SWCNT, and further sonicated by an ultrasonic probe (SONOPULS HD2200, 200W, BANDELIN electronic) for 60 min in an ice bath under argon atmosphere. Subsequently, the solvent was removed under vacuum, and the resulting viscous slurry of Ceraset and P5-SWCNTs placed in a Teflon mold, which was tightly closed by a metal die. The cross-linking was performed at 360 °C for 6 h in an electric furnace (Heraeus) under argon atmosphere. Finally, the samples were subjected to pyrolysis in a quartz tube at 1000 °C for 1 h under argon, with a heating and cooling rate of 10 °C/h and 25 °C/h, respectively. A monolithic ceramic reference sample was prepared from pure Ceraset following the same procedure as described above.

2.2. Morphology

The samples were characterized using a Zeiss GEMINI LEO 1530 VP scanning electron microscope with an acceleration voltage of 3 kV and working distance of 6 mm. For this purpose, the samples were coated by a nominally 0.5 nm thick Pt–Pd layer.

2.3. Mechanical testing

Toward mechanical testing by nanoindentation, a special sample preparation technique [10] was employed. Specifically, plates of 2 mm width and 8 mm length were cut from the circular shaped samples with a diameter of 12 mm, and then mounted into an alumina frame. The platelets were oriented with their side-face upwards, such that a width corresponding to the sample thickness became available for indentation (see inset of Fig. 2a). In the last step, the sample surface was polished to a final roughness of ¼ μm. Vickers indentation of samples was performed with a Buehler Micromet 1 micro indenter (Buehler LTD, Lake Bluff, IL, USA) with an applied load of 1 kg. A representative indentation impression with well-developed radial cracks is shown in Fig. 2a.

Crack profiles were determined with the aid of a scanning electron microscope (Gemini, Zeiss, Germany). The samples were first sputtered with a 0.8 nm thick layer of a gold/palladium alloy.

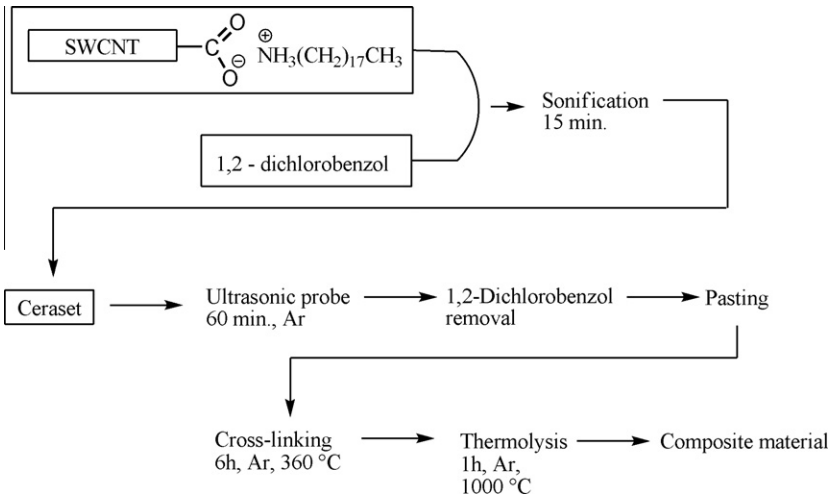

Fig. 1. Synthesis scheme of polymer-derived (Si–C–N) ceramics reinforced by octadecylamine modified SWCNT.

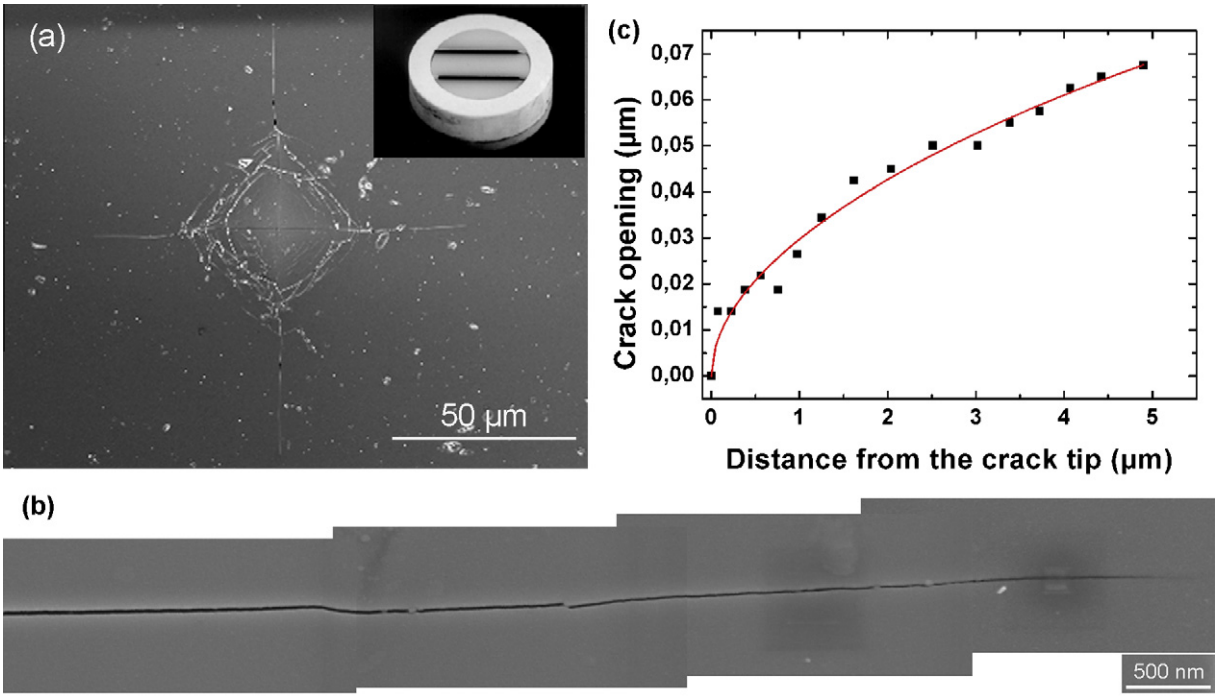

Fig. 2. (a) SEM micrographs of the Vickers indentation impression with associated radial crack system in Si–C–N nanocomposite reinforced by 1 wt.% P5-SWCNTs, the inset on the right represents picture of the sample mounted in the alumina holder, (b) crack tip geometry displayed by an appropriately arranged set of individual SEM images, and (c) crack opening displacement $u(x)$ from the crack tip, data fit (line) is obtained with Eq. (2).

To ensure high reproducibility, in all micrographs the border line between the inner dark region and the white edge region was defined as crack edge position. This was necessary since the edges of the crack faces are not perfectly defined due to deposited carbon contaminations and the sputtered metal. The crack opening along the crack tip was detected by an image assembling procedure (Fig. 2b). In order to remain in the region displaying a parabolic shape of the crack opening displacement (COD) function, data have been collected for the first 5 μm distance from the crack tip. A typical crack opening profile of the crack tip, together with a fitting line obtained using Eq. (2), is presented in Fig. 2c. The plot shows a very good agreement between the fit and the measured data.

The nanoindentation experiments were performed in continuous stiffness mode (CSM) with a Nano Indenter XP nanoindentation system (MTS Nano Instruments, Oak Ridge, TN, USA) and a Berkovich indenter. Since a maximum load of 700 mN is available for this instrument, the penetration depth was limited to 1.6 μm. Nevertheless, the volume of the plastic and elastic deformation field, formed by Berkovich indenter at this penetration depth, is big enough to ensure reliable results [28], as confirmed by reaching plateaus of the measured values already at the penetration depth of 800 nm (Fig. 3). For each sample, the results were averaged over 60 measurements made at five different locations. At each location, a 4×3 array of indentations with a distance of 30 μm was created. Hardness and Young's modulus were determined using the Oliver and Pharr analysis [29]. To this end, the Poisson's ratio value of 0.22, as obtained for pure SiCN pyrolized at 1000 °C [30], was used. Typical values of hardness and Young's modulus obtained in this manner are plotted as a function of tip displacement in Fig. 3. In general, nanoindentation data obtained at small penetration depth are influenced by the surface roughness of the sample. Since the samples were polished to a final roughness of ¼ μm, this influence can be recognized for penetration depths up to 300 nm. Above this range, for both properties there occurs a slight increase, followed by a plateau above 800 nm. The plateau values are expected to be most reliable.

2.4. Electrical conductivity

Electrical conductivity measurements were performed under ambient with a Keithley 2400 source-meter and a DLPCA-200 Femto amplifier. Contact to the samples was made by two needles and silver paste. As four-terminal measurements revealed the presence of only negligible contact resistance mainly two-probe measurements were performed. All I/V curves acquired in the latter configuration generally showed ohmic behavior.

3. Results and discussion

Microstructures at the crack faces for 1 wt.% P-SWCNT/Si–C–N nanocomposites show homogenously distributed carbon nanotubes and plenty of bridging structures reinforcing the enhancement of the mechanical properties (Fig. 4).

SEM micrographs of the fracture surface of the P5-SWCNT-reinforced Si–C–N nanocomposites display a homogeneous distribution of the nanotubes for all three tube contents, as exemplified in Fig. 5. This finding proves the capability of the appended alkyl chains to enhance the interaction with the polymer precursor matrix, which represents a useful extension of previous work on nanocomposites wherein carbon nanotubes are embedded in a polymer-derived ceramic matrix, as has been documented for pristine SWCNTs [24] or MWCNTs [22].

Besides the homogeneous distribution of the nanotubes, the SEM images reveal a similar fracture morphology for both 0.5 and 1 wt.% of P5-SWCNs (Fig. 5a and b), predominately consisting of tubes pulled out from the matrix. In contrast, less pull-out and more broken tubes can be observed for the sample reinforced by 2 wt.% (see Fig. 5c). The different fracture surface morphologies can be explained by an increase of the precursor polymer viscosity due to the addition of the tubes, reflecting in higher carbon nanotube interactions and possibility of their agglomeration. Moreover, owing to the shrinkage of the matrix during pyrolysis, at higher

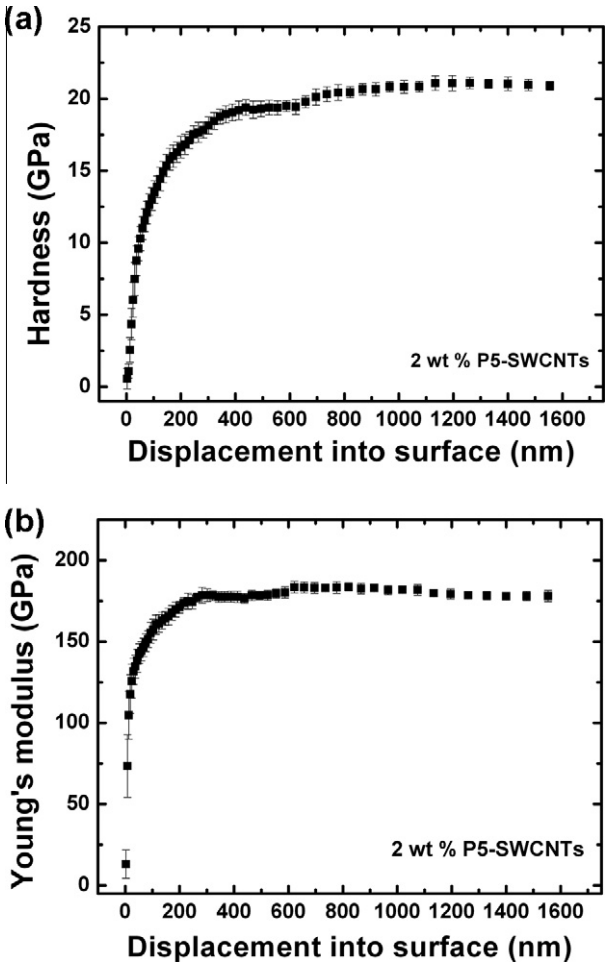

Fig. 3. Plots of (a) hardness and (b) Young's modulus derived via nanoindentation for the polymer-derived Si–C–N nanocomposite reinforced with 2 wt.% P5-SWCNs as a function of penetration depth.

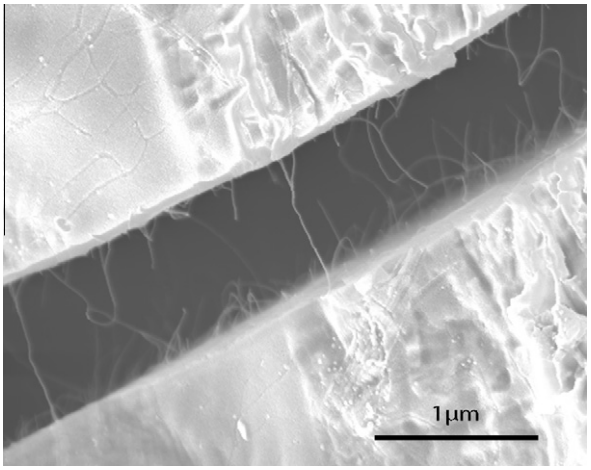

Fig. 4. SEM micrographs at the crack face of the 1 wt.% P-SWCNT/Si–C–N nanocom posites.

nanotube concentrations the tubes are more densely packed, and hence their pull-out more difficult to detect.

Another possible reason for the different fracture surface morphologies relates to the different interfacial strength of tubes and matrix. For fiber-reinforced composites, it is known that the

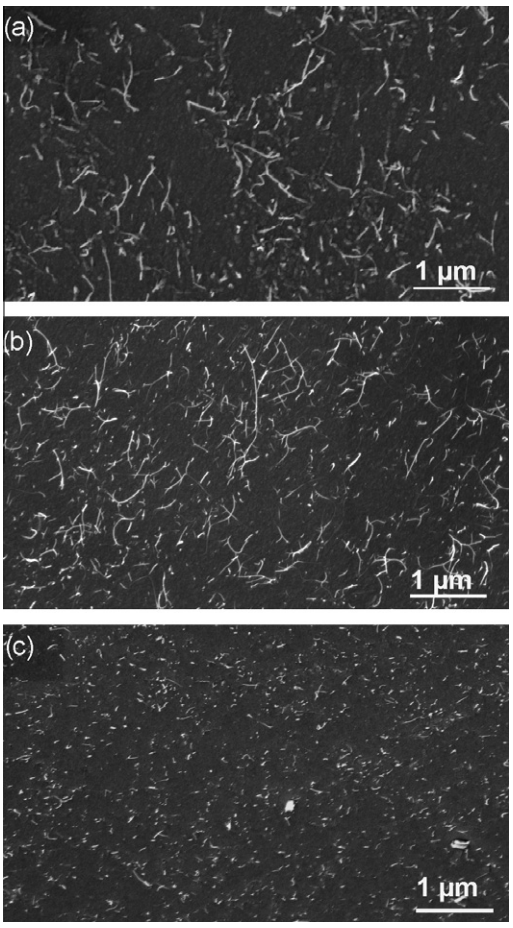

Fig. 5. SEM micrographs of the fracture surfaces of polymer-derived Si–C–N nanocomposite reinforced with (a) 0.5 wt.%, (b) 1 wt.%, and (c) 2 wt.% P5-SWCNs.

ease of pulling-out of fibers from the matrix or their breakage during fracture strongly depends on the interfacial strength of fibers and matrix [31]. Hence, crack deflection along the nanotubes and their subsequent pull-out will be more difficult, with the consequence that the tubes rather break. This explanation gains support from the fracture surface of all three nanocomposites (Fig. 5). In addition, the length and diameter of the fibers, as well as their intrinsic strength and stiffness can have an influence, although these factors are not relevant in our experiments using the same type of tubes. In general, pulling-out of the tubes will be prominent when the tube strength exceeds the interfacial strength, while otherwise they will preferably break.

The values of hardness and Young's modulus, as derived from the nanoindentation load–displacement curves, are plotted in Fig. 6 as a function of the P5-SWCNT content. For the pure polymer-derived Si–C–N ceramic, a Young's modulus of ~141 GPa and a hardness of 17.4 GPa are obtained (see Fig. 6). These values agree well with those reported for polymer-derived Si–C–N ceramics prepared in the same way [23,24]. It can be seen that the incorporation of nanotubes improves both properties in comparison to the pure polymer-derived Si–C–N ceramic. Maximum enhancement is achieved for 2 wt.% tube content, with a value of 182 ± 2 for Young's modulus and 20 ± 0.4 GPa for the hardness. The modulus increase by ~30% is comparable to that observed for the SWCNT reinforcement of polymer-derived-ceramic prepared in the same way [24]. By comparison, the observed hardness by 15% is higher than for the latter material [24].

The enhanced Young's modulus of the reinforced polymer-derived Si–C–N ceramic reflects a sizeable interfacial bonding

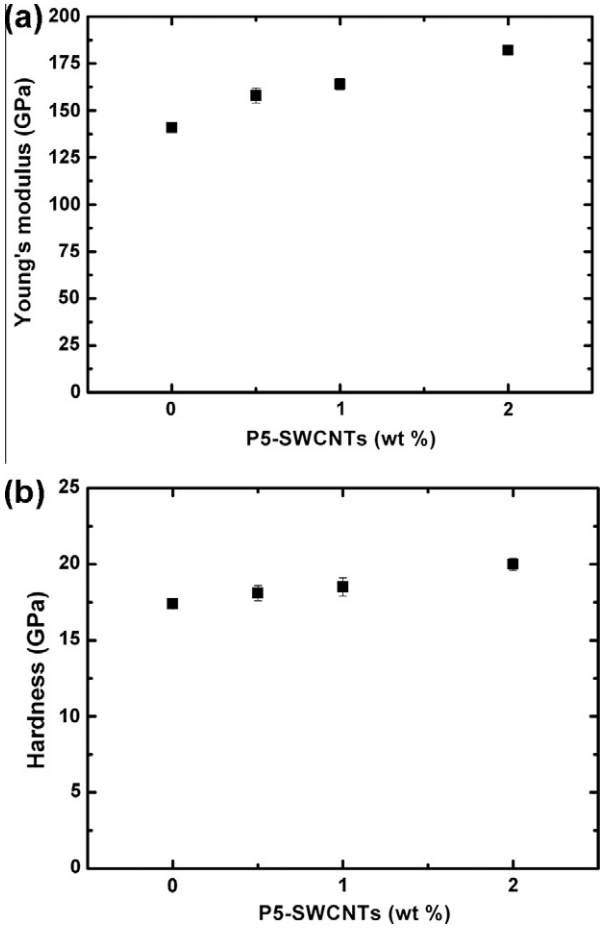

Fig. 6. Dependence of Young's modulus (a) and hardness (b), derived from nanoindentation data of P-SWCNT/polymer-derived Si–C–N ceramic samples with different nanotube content.

strength between the ceramic matrix and the nanotubes, which is an important prerequisite for taking benefit of the exceptionally high Young's modulus of the nanotubes. Such bonding can also be concluded from TEM images of the interface between pristine SWCNTs and polymer-derived ceramics, which reveal good wetting of the ceramic by the tubes, but lack evidence of a strong coupling between these two materials [32]. Therefore, we suppose that chemical bonding between the precursor polymer and nanotubes via functional groups are not present. The octadecylamine modified SWCNT's are soluble in common organic solvents that are compatible with polysilazane, making it possible to prepare those composites by solution-based method. It is furthermore documented that the integrity of the tubes is preserved during pyrolysis at 1000 °C [22,32]. An additional contribution to the enhancement arises from the homogenous distribution of the tubes in the matrix (Fig. 5), which ensures an efficient stress distribution from the matrix to the tubes. It is furthermore noteworthy that the purity of the present tubes is much higher than those in ref [24], which reduces the risk of mechanical failure associated with, e.g., amorphous carbon particles. This can explain the higher hardness of the present composites in comparison to previous studies [24].

Although a direct microscopic proof is lacking, it is nonetheless plausible that the present samples contain SiC nanocrystals at the nanotube/matrix interface, which could exert a positive influence on the properties. Indeed, TEM investigation [22] of Si–B–C–N/CNTs subjected to 1000 °C revealed the nanocrystalline character of the polymer-derived matrix in the vicinity of the tubes. Such template or nucleation effect of CNTs on the matrix crystallization has also been observed for polymer-based CNTs nanocomposites [33,34]. In conclusion, the improved Young's modulus and hardness, as compared to polymer-derived ceramic reinforced by MWCNTs (~120 GPa and ~14 GPa respectively) [21], underline the suitability of the alkyl-functionalized SWCNTs for enhancing the mechanical resilience of these ceramics.

The fracture toughness of the samples was determined through measurement of the crack opening displacement (COD) of indentation cracks in the crack tip vicinity [35,36]. As a major advantage in comparison to the standard crack length measurements [37], this method can be applied to materials showing any type of indentation behavior [10,38]. In fact, the validity of fracture toughness estimation of CNTs/ceramic matrix composites by measuring the crack length using indentation technique has been questioned [39]. By contrast, the COD approach relies upon the crack profile for constant applied load under Mode I conditions, and exploits the fact that the applied stress intensity (K_A) is transferred to the stress field at the crack tip (K_{tip}), while the near-tip half crack opening (u) shows a parabolic dependence on the distance (x) from the crack tip:

$$u(x) = \frac{K_{tip}}{E}\sqrt{\frac{8x}{\pi}} \tag{1}$$

In this equation, K_{tip} is the stress intensity factor at the crack tip, and E is the Young's modulus for plain strain. The K_{tip} value can be obtained by fitting a parabolic profile to the measured crack tip COD as a function of the distance from the crack tip. This approach had originally been developed for compact tension (CT) specimens [35]. When applying it to determine K_{tip} from indentation, however, a complication arises because only a small part of the COD profile close to the crack tip is of parabolic shape [36]. At larger distance from the tip, due to the high residual stress originating from the region near the indent, the parabolic shape can be severely distorted. In order to account for this deviation, a phenomenological fit for the data measured on indentation made cracks has been proposed and proven reliable [10]. The corresponding equation

$$u(x) = \frac{K_{tip}}{E}\sqrt{\frac{8x}{\pi}} + Ax^{\frac{3}{2}} + Bx^{\frac{5}{2}} \tag{2}$$

contains two fitting parameters A and B. Since the present fully dense polymer-derived ceramics reinforced by CNTs can be produced only as small (12 mm diameter) and thin samples (0.45 mm thickness), this fitting method is appropriate [10].

Thus obtained fracture toughness data of the nanocomposites are presented in Fig. 7 as a function of CNT content. The value of 1.4 ± 0.1 MPa $m^{1/2}$ obtained for pure polymer-derived Si–C–N is included as 0 wt.% sample. A more than twofold increase of fracture resistance is observed for all CNTS content in comparison to the pure polymer-derived ceramic.

All three major toughening mechanisms documented for ceramic matrix composites reinforced by micron-scale fibers [40], i.e., crack bridging by fibers, fiber pull-out on the fracture surfaces, and crack deflection at the fiber/matrix interface, are likely to contribute to the toughening in the present samples. Especially the crack deflection mechanism should be operative in light of the high aspect ratio of the used SWCNTs, which represents a critical factor governing the efficacy of crack deflection along the interface [22,23]. Moreover, the tubes' high tensile strength and stiffness is expected to allow effective crack bridging (Fig. 7b and c) and their pull-out (cf. Fig. 5). The relevance of these three mechanisms is further supported by the homogenous distribution of the tubes in the matrix (Fig. 5), which may also explain the smaller fracture toughness of 1.8 MPa $m^{1/2}$ obtained for polymer-derived Si–C–N ceramics reinforced by 2 wt.% of pristine SWCNTs [23]. It is furthermore noteworthy that the fracture

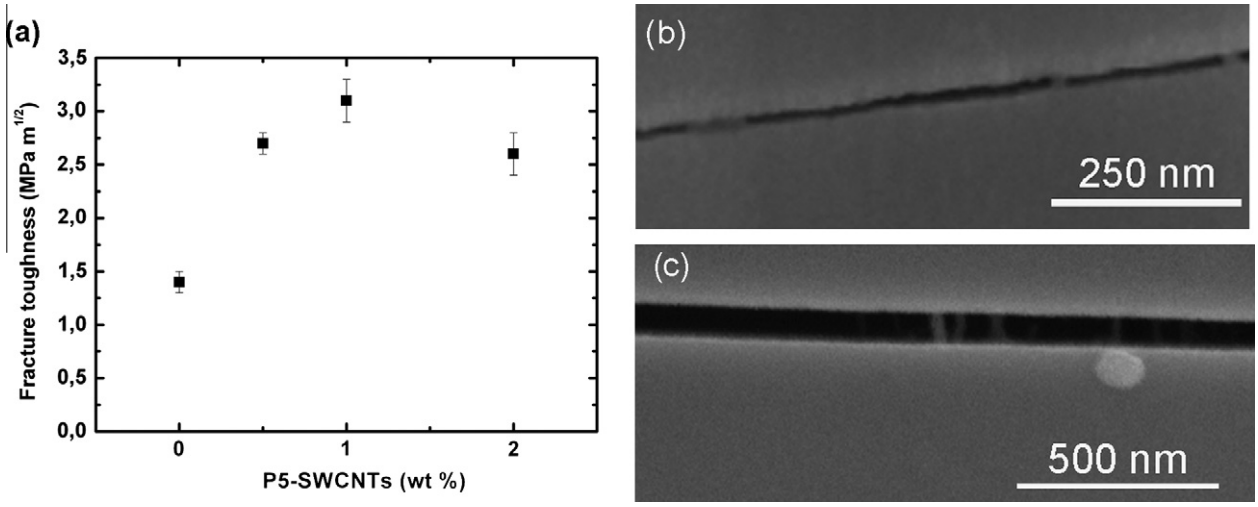

Fig. 7. (a) Dependence fracture toughness extracted from COD data of P-SWCNT/polymer-derived Si–C–N ceramics, on nanotube content; (b and c) examples of crack bridging by CNTs at different distance from the crack tip.

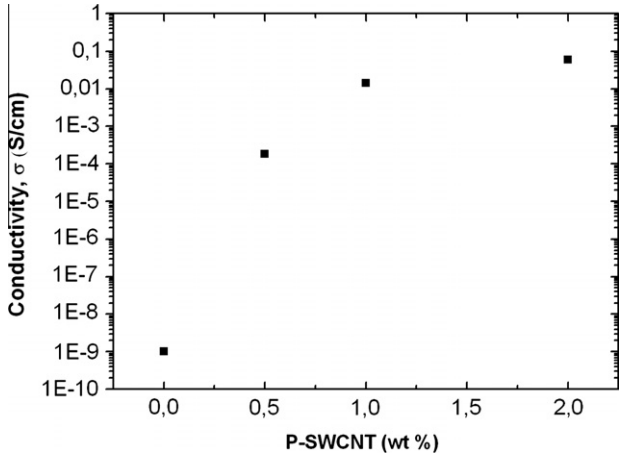

Fig. 8. Dependence of the electrical conductivity of P-SWCNT/Si–C–N ceramic composites on the nanotube content.

toughness does not monotonously increase with rising SWCNT content, but rather displays a maximum of $\sim 3.1 \pm 0.2$ MPa $m^{1/2}$ at 1 wt.%, which is followed by a value of $\sim 2.6 \pm 0.2$ MPa $m^{1/2}$ at the content of 2 wt.%. This trend can be understood on the basis that with increasing content of the tubes, the stiffness and strength of the polymer-derived matrix likewise increases (Fig. 6).

The room temperature electrical conductivity of the pure Si–C–N ceramic pyrolyzed at 1000 °C was found to be 3×10^{-9} S/cm demonstrating its close-to-insolating behavior. Upon incorporation of 0.5 wt.% P5-SWCNTs, the conductivity after pyrolysis increased by five orders of magnitude to 10^{-4} S/cm. As apparent from Fig. 8, the pyrolized specimen display a percolation threshold below 0.5 wt.%, and their conductivity reaches a saturation value of ~0.1 S/cm for a tube content of 2 wt.%. A similar trend has been reported for MWCNT/SiCN composites comprising well-dispersed, non-functionalized nanotubes of high aspect ratio, whereas values >2% are often found in case of CNT/polymer composites [41]. Importantly, the low percolation threshold is not the result of phase segregation, but is rather attained through homogenous dispersion of the P5-SWCNTs within the polymer matrix (see Fig. 5), which is also responsible for the enhanced fracture.

4. Conclusions

In summary, polymer-derived Si–C–N ceramics have been reinforced by alkyl chain-functionalized SWCNTs. We find a remarkably large, more then twofold, increase of fracture resistance in our composites. Furthermore, the incorporation of nanotubes increases the Youngs modulus and hardness of the ceramic matrix by 30%, i.e. 15% (for 2 wt.%), respectively. At the same time, the electrical conductivity is strongly enhanced for tube contents as low as 0.5 wt.%. It is concluded that adequately functionalized SWCNTs are a promising filler material for polymer-derived ceramics, with the potential to obtain composites of high temperature stability as well as excellent toughness and creep resistance.

Acknowledgements

This work is supported within the scope of Schwerpunktprogramm SPP1181 by the Deutsche Forschungsgemeinschaft (DFG). Authors would like to thank to Mr. R. Mager for his assistance in the mechanical testing measurements.

References

[1] Bill J, Aldinger F. Precursor-derived covalent ceramics. Adv Mater 1995;7:775–87.
[2] Thurn G, Canel J, Bill J, Aldinger F. Compression creep behaviour of precursor-derived Si–C–N ceramics. J Euro Ceram Soc 1999;19:2317–23.
[3] Peng JQ, Seifert HJ, Aldinger F. Thermal stability of precursor-derived Si–(B)–C–N ceramics. In: Ceramic transaction 115, proc the American ceramic society's 102nd annual meeting 2000:251.
[4] Zimmermann A, Bauer A, Christ M, Cai Y, Aldinger F. High-temperature deformation of amorphous Si–C–N and Si–B–C–N ceramics derived from polymers. Acta Mater 2002;50:1187–96.
[5] Janakiraman N, Aldinger F. Indentation analysis of elastic and plastic deformation of precursor-derived Si–C–N ceramics. J Eur Ceram Soc 2010;30:775–85.
[6] Müller A, Peng JQ, Seifert HJ, Bill J, Aldinger F. Si–B–C–N ceramic precursors derived from dichlorodivinylsilane and chlorotrivinylsilane. 2. Ceramization of polymers and high-temperature behaviour of ceramic materials. Chem Mater 2002;14:3406–12.
[7] Hörz M, Zern A, Berger F, Haug J, Müller K, Aldinger F. Novel polysilazanes as precursors for silicon nitride/silicon carbide composites without "free" carbon. J Eur Ceram Soc 2005;25:99–110.
[8] Bill J, Kamphowe TW, Mueller A, Wichmann T, Zern A, Jalowieki A, et al. Precursor-derived Si–(B–)C–N ceramics: thermolysis, amorphous state and crystallization. Appl Organomet Chem 2001;15:777–93.
[9] Bauer A, Christ M, Zimmerman A, Aldinger F. Fracture toughness of amorphous precursor-derived ceramics in the silicon–carbon–nitrogen system. J Am Ceram Soc 2001;84:2203–7.
[10] Burghard Z. PhD thesis, University of Stuttgart, Stuttgart; 2004.

[11] Janakiraman N, Burghard Z, Aldinger F. Fracture toughness evaluation of precursor-derived Si–C–N ceramics using the crack opening displacement approach. J Non-Crystall Sol 2009;355:2102–13.
[12] Padtur NP. Multifunctional composites of ceramics and single-walled carbon nanotubes. Adv Mater 2009;21:1767–70.
[13] Cho J, Boccaccini AR, Shaffer MSP. Ceramic matrix composites containing carbon nanotubes. J Mater Sci 2009;44:1934–51.
[14] Treacy MMJ, Ebbesen TW, Gibson JM. Exceptionally high Young's modulus observed for individual carbon nanotubes. Nature 1996;381:678–80.
[15] Wong EW, Sheehan PE, Lieber CM. Nanobeam mechanics: elasticity, strength, and toughness of nanorods and nanotubes. Science 1997;277:1971–4.
[16] Krishnan A, Dujardin E, Ebbesen TW, Yianilos PN, Treacy MMJ. Young's modulus of single-walled nanotubes. Phys Rev B 1998;58:14013–9.
[17] Yu MF, Files BS, Arepalli S, Ruoff RS. Tensile loading of ropes of single wall carbon nanotubes and their mechanical properties. Phys Rev Lett 2000;4:5552–5.
[18] Berber S, Kwon YK, Tomanek D. Unusually high thermal conductivity of carbon nanotubes. Phys Rev Lett 2000;84:4613–6.
[19] Anazawa K, Shimotani K, Manabe C, Wanatabe C, Shimizu M. High-purity carbon nanotubes synthesis method by an arc discharging in magnetic field. Appl Phys Lett 2002;81:739–41.
[20] Cho J, Boccaccini AR, Shaffer MSP. Ceramic matrix composites containing carbon nanotubes. J Mater Sci 2009;44:1934–51.
[21] An LN, Xu WX, Rajagopalan S, Wang CM, Wang H, Fan Y. Carbon-nanotube-reinforced polymer-derived ceramic composites. Adv Mater 2004;16:2036–40.
[22] Katsuda Y. PhD thesis, University of Stuttgart; 2006.
[23] Katsuda Y, Gerstel P, Narayanan J, Bill J, Aldinger F. Reinforcement of precursor-derived Si–C–N ceramics with carbon nanotubes. J Am Ceram Soc 2006;26:3399–405.
[24] Burghard Z, Schon D, Bill J, Aldinger F. Polymer-derived Si–C–N ceramics reinforced by single wall carbon nanotubes. Int J Mater Res 2006;97:1667–72.
[25] Li Y, Fernandez-Recio L, Gerstel P, Srot V, van Aken PA, Kaiser A, et al. Chemical modification of single-walled carbon nanotubes for the reinforcement of precursor-derived ceramics. Chem Mater 2008;20:5593–9.
[26] Gojny FH, Nastalczyk J, Roslaniec Z, Schulte K. Surface modified carbon nanotubes in CNT/epoxy-composites. Chem Phys Lett 2003;370:820–4.
[27] Hill DE, Lin Y, Allard LF, Sun Y. Solubilisation of carbon nanotubes vie polymer attachment. Int J Nanosci 2002;3(4):213–21.
[28] Bhushan B, Li X. Nanomechanical characterisation of solid surfaces and thin films. Int Mater Rev 2003;48:125–64.
[29] Oliver WC, Pharr GM. An improved technique for determining hardness and elastic modulus using load and displacement sensing indentation experiments. J Mater Res 1992;7:1564–83.
[30] Janakiraman N, Aldinger F. Fabrication and characterization of fully dense Si–C–N ceramics from a poly(ureamethylvinyl)silazane precursor. J Eur Ceram Soc 2009;29:163–73.
[31] Steen M, Valles JL. Interfacial bond conditions and stress distribution in a 2-D reinforced brittle matrix composite. Compos Sci Technol 1998;58:313–30.
[32] Cai Y, Shah SR, Zimmermann A, Weinmann M, Raj R, Aldinger F. Carbon nanotubes welded by precursor derived silicoboron carbonitride ceramics. Phys Status Solidi A 2002;193:R13–5.
[33] Valentinia L, Biagiottia J, Kenny JM, Santucci S. Morphological characterization of single-walled carbon nanotubes-PP composites. Compos Sci Technol 2003;63:1149–53.
[34] Probst O, Moore EM, Resasco DE, Grady BP. Nucleation of polyvinyl alcohol crystallization by single-walled carbon nanotubes. Polymer 2004;45:4437–43.
[35] Rödel J, Kelly JF, Lawn BR. In situ measurements of bridged crack interfaces in the SEM. J Am Ceram Soc 1990;72:3313–8.
[36] Seidel J, Rödel J. Measurement of crack tip toughness in alumina as a function of grain size. J Am Ceram Soc 1997;80:433–8.
[37] Anstis GR, Chanticul P, Lawn BR, Marshall DB. A critical evaluation of indentation techniques for measuring fracture toughness: I, direct crack measurements. J Am Ceram Soc 1981;64:533–8.
[38] Burghrad Z, Zimmerman A, Aldinger F, Rödel J, Lawn BR. Crack opening profiles of indentation cracks in normal and anomalous glasses. Acta Mater 2004;52:293–7.
[39] Sheldon BW, Curtin WA. Nanoceramic composites: tough to test. Nat Mater 2004;3:505–6.
[40] Curtin WA. Dimensionality and size effects on the strength of fiber-reinforced composites. Compos Sci Technol 2000;60:543–51.
[41] Ionescu E, Francis A, Riedel R. Dispersion assessment and studies on AC percolative conductivity in polymer-derived Si–C–N/CNT ceramic nanocomposites. J Mater Sci 2009;44:2055–62.